VLDL-triglyceride production after alcohol ingestion, studied using [2-$^{13}C_1$] glycerol

Scott Q. Siler,* Richard A. Neese,*,† Elizabeth J. Parks,* and Marc K. Hellerstein[1,*,†]

Department of Nutritional Sciences,* 309 Morgan Hall, University of California at Berkeley, CA 94720-3104; and Division of Endocrinology and Metabolism,† Department of Medicine, University of California, San Francisco, 1001 Potrero Avenue, San Francisco, CA 94110

Abstract **We used [2-$^{13}C_1$]glycerol to characterize very low density lipoprotein (VLDL)-triglyceride kinetics and intrahepatic glycerol metabolism in normal men (n = 4) after alcohol (EtOH) ingestion. [2-$^{13}C_1$]glycerol was infused before and after the consumption of 48 g EtOH or a placebo. Three additional subjects also received [1-$^{13}C_1$]acetate in addition to the [2-$^{13}C_1$]glycerol with EtOH treatment. Incorporation of tracer into the glycerol or fatty acid moiety of VLDL-triglyceride was measured by gas chromatography–mass spectrometry and used to calculate VLDL-triglyceride production rates. Intrahepatic triose-phosphate enrichments were also calculated based on mass isotopomer distribution analysis of plasma glucose. There was no difference in VLDL-triglyceride production rates after 48 g EtOH (11.9 ± 3.7 mg/kg/h) or placebo (14.7 ± 3.3 mg/kg/h). The VLDL-triglyceride rate constants calculated by kinetic modeling using the glycerol and acetate tracers in the combined isotope infusion subjects were very closely correlated (r^2 = 0.94). The peak VLDL-glycerol enrichments after EtOH were 22.5 ± 3.3% versus 7.6 ± 0.8% after placebo ($P <$ 0.001), while intrahepatic triose-phosphate enrichments were 19.8 ± 1.3% and 13.1 ± 1.2% ($P <$ 0.001), respectively. Moreover, the calculated asymptotic VLDL-glycerol enrichments (representing the hepatic α-glycerol phosphate enrichment) were significantly higher after EtOH than placebo. The higher ratio of VLDL-glycerol to triose-phosphate labeling after EtOH suggests a metabolic block at glycerol 3-phosphate dehydrogenase. We conclude that consumption of 48 g EtOH does not increase VLDL-triglyceride production in normal men but does cause accumulation of tracer in hepatic α-glycerol phosphate.—**Siler, S. Q., R. A. Neese, E. J. Parks, and M. K. Hellerstein. **VLDL-triglyceride production after alcohol ingestion studied using [2-$^{13}C_1$]glycerol. *J. Lipid Res.* 1998.** 39: **2319–2328.**

Supplementary key words MIDA • alcohol • glycerol phosphate • hypertriglyceridemia • kinetic modeling

The consumption of alcohol (or ethanol, EtOH) has been reported to acutely increase serum triglyceride (TG) concentrations in healthy volunteers, particularly when large doses (>50 g) are administered (1–5). Hypertriglyceridemia has also been observed in some individuals who consume large quantities of EtOH regularly (6, 7). Hypertriglyceridemia is usually associated with an increased risk of coronary heart disease (8), but regular EtOH intake is not associated with increased risk (9, 10). Mechanistic observations on the triglyceridemic response to EtOH may help us to better understand these relationships and the clinical implications of EtOH-induced hypertriglyceridemia.

Increased serum TG levels can result from increased production and/or reduced clearance of very low density lipoprotein (VLDL)-TG. Overproduction of VLDL-TG has been shown to contribute to hypertriglyceridemia syndromes in other settings not associated with EtOH intake (11, 12), but there are some discrepancies in the literature as to whether VLDL-TG production is elevated by EtOH. Some studies have found an increased VLDL-TG production in persons exposed to EtOH (13–16), while others have not (13, 16, 17). Plasma clearance of TG may also play a role in increasing serum TG after EtOH, as TG clearance has been reported to be either increased (14–16) or unchanged by EtOH intake (7, 13). Additionally, EtOH has been shown to delay the clearance of dietary TG (13).

The goal of this study was to characterize the kinetic response of serum triglycerides to acute EtOH consump-

Abbreviations: EtOH, ethanol; TG, triglyceride; VLDL, very low density lipoprotein; BIA, bioelectrical impedance analysis; LBM, lean body mass; GC-MS, gas chromatography–mass spectrometry; MeOH-HCl, methanolic hydrochloric acid; FAME, fatty acid methyl esters; M_0, M+0 isotopomer; M_1, M+1 isotopomer; M_2, M+2 isotopomer; MIDA, mass isotopomer distribution analysis; Ra, rate of appearance; DNL, de novo lipogenesis; GNG, gluconeogenesis; ΔA_1, change in fractional abundance of M+1 isotopomer; ΔA_2, change in fractional abundance of M+2 isotopomer; K_s, rate constant of rise to plateau; A_∞, plateau value of glycerol enrichment or fractional DNL based on kinetic modeling; ANOVA, analysis of variance; BAC, blood alcohol concentration; K_d, rate constant of removal; FFA, free fatty acids; NADH, reduced nicotinamide adenine dinucleotide; NAD, nicotinamide adenine dinucleotide; DHAP, dihydroxy acetone phosphate; G3PDH, glycerol 3-phosphate dehydrogenase; BMI, body mass index; HDL, high density lipoprotein; $t_{1/2}$, fractional half-life; MPE, mole percent excess; p, precursor enrichment; Glc, glucose; GAP, glyceraldehyde 3-phosphate; Gly-3P, glycerol 3-phosphate; Gly, glycerol; AcCoA, acetyl-coenzyme A, FA-CoA, fatty-acyl-CoA; Ac, acetate; FA, fatty acid; AcHO, acetaldehyde.

[1]To whom correspondence should be addressed.

tion. We measured VLDL-TG production based on the incorporation of [2-$^{13}C_1$]glycerol in young, healthy volunteers after the consumption of 48 g EtOH or a placebo. In addition, we performed a study in a subset of subjects to compare this method to the incorporation of [1-$^{13}C_1$]acetate into VLDL-TG, as the latter has been used by us (17, 18) and others (19) previously as a technique for the measurement of VLDL-TG production rate. Aspects of glycerol metabolism in plasma and liver are also reported.

METHODS

Materials

[2-$^{13}C_1$]glycerol and [1-$^{13}C_1$]acetate were purchased from CIL (Andover, MA) and/or Isotec (Miamisburg, OH). Isotopic purity was greater than 98% for all tracers used.

Subject characteristics

Volunteers (n = 7) were recruited by advertisement and gave informed consent before enrolling in the study. All protocols were approved by the University of California at San Francisco and Berkeley Committees on Human Research. All subjects were males and moderate consumers of EtOH (<120 g/week). None of the subjects had any history of alcoholism, and all subjects had normal lipid profiles and liver enzyme concentrations in serum. None of the subjects had any history of medical diseases, metabolic disorders, or were using any medications with known metabolic effects. Additionally, none of the subjects had diabetes mellitus, nor did they have any family history of diabetes. Subject characteristics are shown in **Table 1**. Body composition was measured by bioelectrical impedance analysis (BIA, Model #1990B, Valhalla Scientific Inc., San Diego, CA). Body fat and total body water were calculated according to the manufacturer's equations.

Study design

Four subjects were admitted twice to the General Clinical Research Center at San Francisco General Hospital for separate studies. During one admission, 4 alcoholic beverages containing 12 g EtOH (40% vodka, Absolut, Ahus, Sweden) mixed with sugar-free lemonade (Kraft General Foods, White Plains, NY) were administered; during the other admission, the sugar-free lemonade was given as a placebo. Each EtOH cocktail contained 84 kcal from EtOH and 4 kcal from the sugar-free lemonade, while the placebo cocktails contained 4 total kcal (as measured by bomb calorimetry). The order of the treatment was randomized, with the second admission following 1 week after the first.

The infusion protocol was as follows. After an evening meal (40% total daily caloric requirement, 55/30/15, carbohydrate/fat/protein) at 1700, a constant intravenous infusion of [2-$^{13}C_1$]-glycerol (0.25 mg/kg LBM/min) was begun at 0500. The infusion continued until 1300, at which time subjects were again allowed access to food. Cocktails (EtOH or placebo) were administered at 0800, 0830, 0900, and 0930. Blood was drawn before tracer administration (baseline), in the hour before the cocktails (pre-EtOH), and half-hourly thereafter.

An additional study was performed in three subjects to validate the method of using [2-$^{13}C_1$]-glycerol incorporation into VLDL-TG as a means to quantify VLDL-TG production. These subjects participated only in the EtOH phase; no placebo phase was adminstered. The infusion paradigm was similar to that described above, with the following modifications. [1-$^{13}C_1$]acetate (1 g/h) was infused at a constant rate from 0400 to 1400 in addition to the [2-$^{13}C_1$]glycerol (0.25 mg/kg LBM/min) that was infused from 0500 to 1300. EtOH cocktails (12 g EtOH in sugar-free lemonade) were administered at 0800, 0830, 0900, and 0930. Blood was drawn before tracer administration (baseline), in the hour before the cocktails (pre-EtOH), and half-hourly thereafter. No other food was consumed during the study.

Metabolite isolation and measurement

Blood alcohol concentrations were measured using a standard kit (Sigma, St. Louis, MO). Plasma TG concentrations were measured enzymatically using a Ciba Corning Express 550 automated analyzer (Chiron, Emeryville, CA).

Plasma glycerol and glucose were isolated by ion-exchange chromatography as described previously (20–22). Plasma was deproteinized with perchloric acid (1:2), neutralized with 6 N KOH, and loaded with a water wash onto gravity flow columns. One set of columns contained an anion exchange resin (AG 1-X8 Bio-Rad, Hercules, CA) and the other contained a cation exchange resin (AG 50W-X8 Bio-Rad, Hercules, CA). The two columns were used in sequence, with the eluent collected completely and lyophilized. The samples were then divided and derivatized in one of two ways. The tri-acetate derivative was used for the glycerol fraction. One hundred μl of acetic anhydride–pyridine 2:1 was allowed to react with the lyophilized sample at room temperature for 15 min. After drying under nitrogen gas, the sample was reconstituted in ethyl acetate for GC-MS analysis. The glucose fraction of the ion exchange column eluent was derivatized to the aldonitrile tetraacetate derivative. Hydroxylamine in pyridine (2%) was reacted with the lyophilized sample for 30 min at 100°C. Twenty-five μl of acetic anhydride–pyridine 2:1 was added after cooling and allowed to react for 15 min at room temperature. The solution was then reconstituted in ethyl acetate after drying under nitrogen gas.

VLDL were isolated by ultracentrifugation as described previously (23). The isolated VLDL were extracted according to Folch, Lees, and Sloane Stanley (24). After evaporation to dryness of the extracted VLDL lipids, 1 ml each of chloroform and 3.0 N MeOH-HCl were added and allowed to react at room temperature overnight. The fatty acid methyl esters (FAME) were extracted twice with hexane after the addition of 5% NaCl. The extracted FAME were evaporated to dryness under N_2 gas and resuspended in heptane for GC-MS analysis. The aqueous component (containing TG-glycerol) was also evaporated to dryness under N_2 gas. This portion was then derivatized as described above for glycerol. This method for VLDL extraction does not isolate TG exclusively; phospholipids and cholesteryl esters are also extracted. Thus, our analyses of VLDL-glycerol and VLDL-palmitate

TABLE 1. Subject characteristics

	Age	Weight	BMI	Body Fat	LBM	Total Body Water	Serum Triglycerides	Serum Total Cholesterol	Serum HDL Cholesterol
	yr	*kg*	*kg/m²*	*%*	*kg*	*L*	*mg/dl*	*mg/dl*	*mg/dl*
Mean ± SD	27.1 ±1.6	78.0 ± 6.8	24.3 ± 2.2	12.4 ± 3.2	67.0 ± 6.3	54.0 ±10.9	107 ± 43	154 ± 28	42 ± 12

n = 7. See text for details. Abbreviations: BMI, body mass index; LBM, lean body mass; HDL, high density lipoprotein.

represent input from a mixture of TG, phospholipid, and cholesteryl ester. The composition of each component is as follows (25). Glycerol derived from TG contributes 72.4% of the total glycerol in VLDL, while the remaining 27.6% is present in the phospholipid component. Fatty acids from TG, phospholipids, and cholesteryl ester contribute 74.3%, 18.9%, and 6.8% of the total fatty acids present in VLDL, respectively. As TG contributes the bulk of glycerol and fatty acids to the VLDL particle, we have expressed the changes that we observe in VLDL-glycerol and VLDL-palmitate as representing primarily changes in VLDL-TG.

Mass spectrometry

Gas chromatography–mass spectrometry (GC-MS) was performed using an HP 5971 instrument (Hewlett-Packard, Palo Alto, CA) in the selected-ion monitoring mode to determine the isotopic enrichments of glycerol (26), aldonitrile-glucose, and palmitate-methyl ester (26). For glycerol and aldonitrile-glucose, chemical ionization mode was used; palmitate-methyl esters were analyzed with electron-impact ionization. A 10 m DB225 (J&W Scientific, Folsom, CA) column was used for GC-MS analysis of the glycerol-triacetate with the initial temperature 75°C and rising 45°C/min to 160°C, 5°C/min to 171°C, and 40°C/min to a final temperature of 220°C. The M_0 and M_1 of m/z 159 and 160 were collected. The aldonitrile tetraacetate derivative of glucose was analyzed using a 60 m DB17 GC column (J&W Scientific, Folsom, CA). The initial temperature rose from a starting value of 120°C to a final temperature of 270°C at a rate of 40°C/min; the oven was held at 270°C for 7 min. The ions monitored were m/z 328, 329, and 330 (M_0, M_1, and M_2). A 40 m DB-1 (J&W Scientific, Folsom, CA) column was used for chromatographic separation of palmitate-methyl esters. The initial temperature started at 80°C and rose 40°C/min to 310°C followed by a rise to 325°C at a rate of 3°C/min. The M_0 of m/z 270, M_1 of 271, and M_2 of 272 were collected.

Calculations

The rate of appearance (Ra) of plasma glycerol was calculated by the dilution technique (18, 27), using non-tracer dose of glycerol (see Discussion). The rate of appearance of glycerol was calculated from both pre-EtOH/placebo and post-EtOH/placebo timepoints. Values from the 0740, 0750, and 0800 samples were used for the pre-EtOH/placebo measurements and steady-state values between 0900–1200 were used for the post-EtOH/placebo measurements. Mass isotopomer distribution analysis (MIDA) was used to calculate the fractional contribution from de novo lipogenesis to the VLDL-palmitate pathway (fractional DNL, references 28–30), fractional gluconeogenesis (GNG, reference 22), and the isotopic enrichment of the precursor of each (hepatic acetyl-CoA and triose-phosphate, respectively, references 22, 28–30). Based on the principal of combinatorial probabilities, the enrichment of the true precursor (acetyl-CoA for DNL, triose-phosphate for GNG) was inferred from the ratio of the excess double-labeled to single-labeled species ($\Delta A_2/\Delta A_1$) of each molecule. The precursor–product relationship was then used to calculate the fractional contribution of de novo lipogenesis to the VLDL fatty acids or gluconeogenesis to glucose production. More detailed explanations of the MIDA calculations are presented elsewhere (31). The hepatic triose-phosphate enrichments calculated from plasma glucose by MIDA can be compared to enrichments in VLDL-TG glycerol, as the latter is derived from hepatic α-glycerol phosphate (**Fig. 1**).

VLDL-TG production was calculated by modeling the rise towards plateau in VLDL-glycerol enrichment from [2-$^{13}C_1$] glycerol and/or in newly synthesized VLDL-palmitate from [1-$^{13}C_1$]-acetate incorporation (fractional DNL, 17–19). VLDL-glycerol enrichment values from half-hourly samples between 800 and 1300 and fractional DNL values from half-hourly samples from 800 to 1400 were plotted, and the best fit for the curve of each versus time was calculated using the Sigma Plot

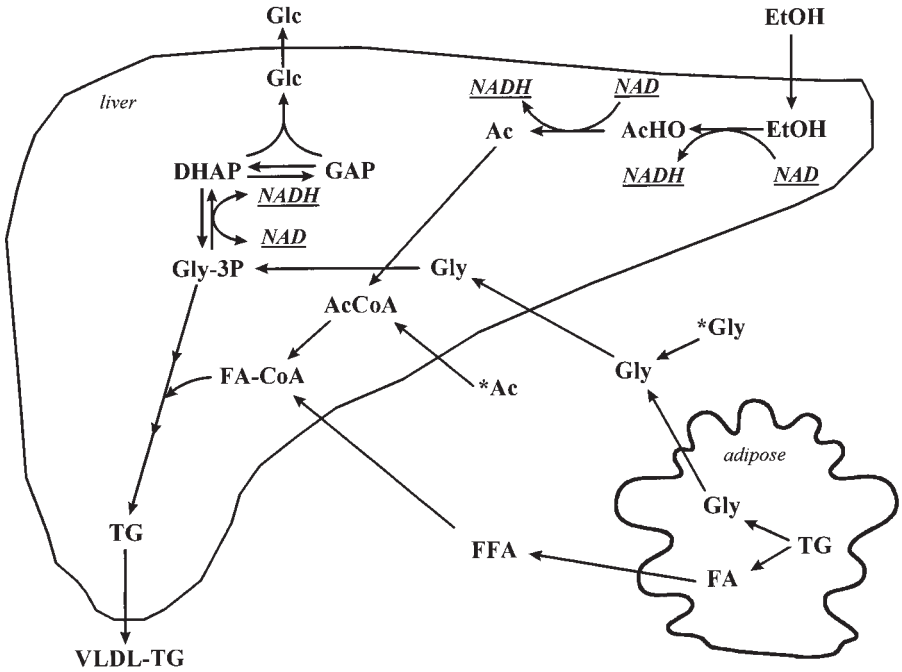

Fig. 1. Key pathways of glycerol metabolism and VLDL-TG synthesis in response to EtOH. Abbreviations used: glc, glucose; DHAP, dihydroxyacetone phosphate; GAP, glyceraldehyde 3-phosphate; gly-3P, α-glycerol phosphate; gly, glycerol; AcCoA, acetyl-coenzyme A; FA-CoA, fatty acyl-coenzyme A; TG, triglyceride; VLDL-TG, very low density lipoprotein-triglyceride; EtOH, ethanol; AcHO, acetaldehyde; Ac, acetate; FFA, free fatty acid; FA, fatty acid; NAD, nicotinamide adenine dinucleotide; NADH, reduced nicotinamide adenine dinucleotide; (*) denotes a ^{13}C-labeled metabolite.

computer program (Jandel Scientific, San Rafael, CA). The data were fit to the equation $y = A_\infty \cdot (1-e^{-Ks(t-c)})$ where y = VLDL-glycerol enrichment or fractional DNL, A_∞ = the plateau value of TG-glycerol or fractional DNL, K_s (hr^{-1}) = the rate constant of rise to plateau in VLDL-TG, t = time in hours, and c = the lag period before isotope incorporation into secreted VLDL-TG. VLDL-TG production was then calculated as K_s (hr^{-1}) × pool size (mg), where pool size = average TG concentration (mg/dl) × estimated plasma volume (5% of total body weight). VLDL-TG half life was calculated by dividing 0.69 by K_s.

Statistics

All results are presented as means ± standard deviation. Two-factor repeated measures analysis of variance (ANOVA) with time and treatment as the two trial factors were performed for most parameters. Statistical differences in VLDL-TG production rates, K_s, and A_∞ were calculated using a matched, paired *t*-test. None of the values for the three combined isotope infusion study subjects were included in any of the statistical analyses except for DNL, which was measured only in this study. DNL and EtOH concentrations were analyzed only for a time effect. Tukey's post-hoc test was used to determine statistical significance ($P < 0.05$) for all parameters analyzed by ANOVA.

RESULTS

Plasma concentrations of metabolites

Blood alcohol concentrations (BAC) rose from undetectable levels at 0800 to a peak of 14.5 ± 3.6 mm at 1000 (**Fig. 2**). BAC decayed linearly thereafter and was 6.6 ± 2.6 mm at the end of the study (1300). Plasma TG concentrations rose 43 ± 21% ($P < 0.01$) after EtOH, from a pre-EtOH mean of 112 ± 78 mg/dl to 150 ± 78 mg/dl at 1300 (**Fig. 3**). The average value over the course of the study was 118 ± 67 mg/dl (**Table 2**). Plasma TG concentrations fell 2 ± 18% in the placebo treatment (119 ± 38 mg/dl pre-placebo, 115 ± 42 mg/dl at 1300); the average value over time was 111 ± 31 mg/dl (Table 2).

Plasma glycerol enrichment and flux

Plasma glycerol enrichments (%) showed a trend towards an increase after EtOH and decrease after the placebo (**Table 3**), although none of the differences reached statistical significance. The mean plasma glycerol flux (the rate of appearance of glycerol) decreased 25% (not significant, $P = 0.07$) after EtOH from a baseline value of 2.64 ± 0.72 μmol/kg per min to 1.98 ± 0.87 μmol/kg per min (**Table 4**). In contrast, the rate of appearance of glycerol increased 17% ($P = 0.07$) from a pre-placebo value of 2.54 ± 0.50 μmol/kg per min to 2.96 ± 0.51 μmol/kg per min following consumption of the placebo.

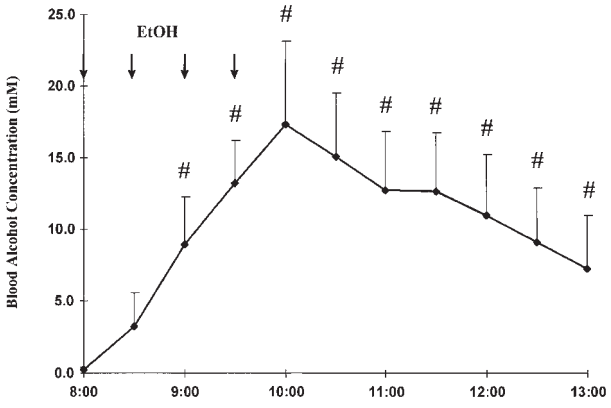

Fig. 2. Blood alcohol concentrations; #statistically significant difference vs. pre-EtOH (8:00) values.

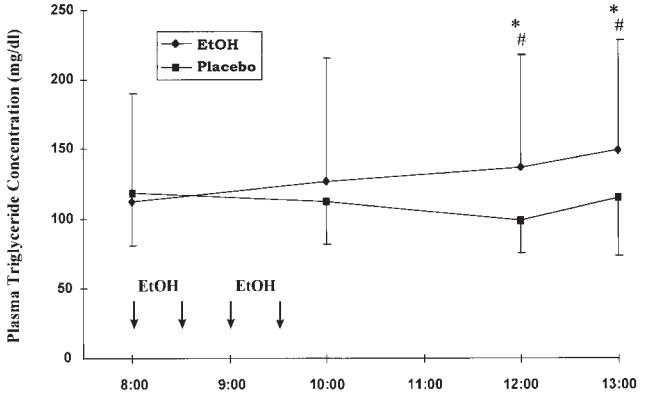

Fig. 3. Plasma triglyceride concentrations after EtOH or placebo; *statistically significant difference between treatments; #statistically significant difference vs. pre-treatment values.

VLDL-glycerol and hepatic triose-phosphate enrichment

VLDL-glycerol enrichments rose over time in both the placebo and EtOH studies (**Fig. 4**, Table 3). The initial measurement of VLDL-glycerol enrichment at 0740 in the placebo study was 2.3 ± 1.2%; the final measurements between 1130 and 1300 were 6.8 ± 1.0% to 7.6 ± 0.8%. The 0740 VLDL-glycerol value was similar in the EtOH study (2.9 ± 1.0%), but the 1130 to 1300 values (18.9 ± 2.9% to 22.5 ± 3.3%) were very different ($P < 0.001$). Thus, EtOH initiated a dramatic and statistically significant increase in VLDL-glycerol enrichments as compared to both pre-EtOH and placebo values (Fig. 4).

Hepatic triose-phosphate enrichments calculated by MIDA from plasma glucose also increased after EtOH (Table 3 and **Table 5**). The pre-EtOH value was 12.2 ± 1.4% and increased after EtOH to 19.8 ± 1.3% at 1300. Triose-phosphate enrichments were unchanged from baseline after the placebo, the average value being 12.7 ± 1.1%. Post-EtOH triose-phosphate values from 0900 to 1300 were significantly different than the placebo and the pre-EtOH values.

Fractional de novo lipogenesis

Fractional DNL was measured in the three subjects who participated in the combined label portion of this study (**Fig. 5**, **Table 6**). The average baseline value was 10 ± 10% and it rose to a final value of 37 ± 7% at 1400 ($P < 0.001$). One of the three subjects had an unusually high baseline value (20%), adding to the large standard deviation observed for the baseline values. All three fractional

TABLE 2. VLDL-TG production rates and other measures after EtOH or placebo treatment

	EtOH				Placebo			
Subject	K_s	$t_{1/2}$	Plasma TG Concentration	VLDL-TG Production Rate	K_s	$t_{1/2}$	Plasma TG Concentration	VLDL-TG Production Rate
	h^{-1}	*h*	*mg/dl*	*mg/kg/h*	h^{-1}	*h*	*mg/dl*	*mg/kg/h*
1	0.19	3.58	75	7.3	0.33	2.12	71	11.6
2	0.28	2.42	81	11.5	0.36	1.92	102	18.4
3	0.12	5.91	250	14.6	0.24	2.82	134	16.4
4	0.28	2.49	120	16.6	0.18	3.84	138	12.4
Mean	0.21	3.6	118	11.9	0.28	2.7	111	14.7
± SD	0.07	0.9	67	3.7	0.08	0.9	31	3.3

Conditions and calculations are as described in the text. Kinetics are based on [2-$^{13}C_1$]glycerol incorporation. Individual data compare EtOH versus placebo treatments. Values are means ± SD. There were no statistically significant differences observed between the EtOH and placebo treatments for any of the parameters listed. Abbreviations used: K_s, synthetic constant; $t_{1/2}$, half-life; TG, triglyceride; VLDL-TG, very low density lipoprotein-triglyceride.

DNL curves were modeled to calculate kinetics of VLDL-TG. The DNL precursor enrichment values fell after the consumption of the EtOH; the initial 0800 value was 0.092 ± 0.013 and the steady-state post-EtOH value was 0.041 ± 0.004.

Kinetic modeling and calculation of triglyceride fluxes

Modeling the rate of the rise toward plateau of VLDL-glycerol enrichment in the EtOH and placebo studies enabled us to calculate several VLDL-TG kinetic parameters (Table 2 and **Table 7**). The mean K_s was 0.21 ± 0.07 hr^{-1} in the EtOH study and 0.28 ± 0.08 hr^{-1} in the placebo study (Table 2). Thus, the half-life of VLDL-TG was 3.6 ± 1.4 h in the EtOH study and 2.7 ± 0.9 h in the placebo study (Table 2). There were no statistically significant differences between the two treatments for K_s or $t_{1/2}$. The predicted mean asymptotic VLDL-glycerol enrichment (A_∞) from the curve-fitting was 41.0 ± 4.0% in the EtOH study and 9.2 ± 1.4% in the placebo study ($P < 0.01$, Fig. 4).

In the three subjects participating in the methodological comparison phase of the study, K_s was calculated after EtOH consumption by independently modeling the incorporation of [1-$^{13}C_1$]acetate and [2-$^{13}C_1$]glycerol into VLDL-TG (Table 7). For [1-$^{13}C_1$]acetate, the rate of rise toward plateau of label incorporation into newly synthesized palmitate molecules (fractional DNL) was modeled. The average K_s value calculated by the modeling of [1-$^{13}C_1$]acetate incorporation into newly synthesized VLDL-TG palmitate was 0.20 ± 0.08 h^{-1} and by the modeling of [2-$^{13}C_1$]glycerol incorporation into VLDL-TG was 0.20 ± 0.07 h^{-1}.

The mean VLDL-TG production rate was 11.9 ± 3.7 mg/kg per h in the EtOH study and 14.7 ± 3.3 mg/kg per h in the placebo study, using the [2-$^{13}C_1$]glycerol results. Individual data are listed in Table 2. There were no statistically significant differences between the two treatments. When VLDL-TG production was calculated using the [1-$^{13}C_1$]acetate incorporation into newly synthesized palmitate

TABLE 3. Isotopic enrichments of plasma glycerol and products derived from glycerol during EtOH or placebo studies

	EtOH				Placebo			
Time	Plasma Glycerol Enrich.	VLDL-Glycerol Enrich.	Hepatic Triose-P Enrich.	Time	Plasma Glycerol Enrich.	VLDL-Glycerol Enrich.	Hepatic Triose-P Enrich.
	mol % excess				*mol % excess*		
0740	53.4 ± 10.4	2.9 ± 1.0	12.2 ± 1.4	0740	47.5 ± 6.7	2.3 ± 1.2	12.9 ± 1.9
0800	48.8 ± 7.5	3.5 ± 1.1	12.1 ± 1.0	0800	47.5 ± 8.4	3.1 ± 1.2	12.6 ± 1.3
0830	53.0 ± 7.9	3.8 ± 0.9	12.5 ± 1.2	0830	45.2 ± 16.3	3.8 ± 1.2	12.3 ± 1.2
0900	57.0 ± 7.5	5.0 ± 1.8	14.0 ± 1.4[ab]	0900	49.9 ± 11.8	4.5 ± 1.0	12.3 ± 1.3
0930	56.1 ± 8.2	8.5 ± 2.1[a]	14.8 ± 1.9[ab]	0930	56.0 ± 7.7	4.9 ± 0.9	12.4 ± 1.1
1000	55.4 ± 10.2	11.1 ± 4.6[a]	15.5 ± 2.3[ab]	1000	47.3 ± 15.2	5.6 ± 1.0	12.1 ± 1.0
1030	65.4 ± 9.3	14.0 ± 3.3[ab]	16.6 ± 1.4[ab]	1030	48.3 ± 10.0	5.4 ± 0.6	12.2 ± 0.9
1100	62.3 ± 12.1	17.4 ± 3.9[ab]	17.3 ± 1.2[ab]	1100	44.1 ± 11.1	6.4 ± 1.1	12.5 ± 0.8
1130	59.3 ± 12.7	18.9 ± 2.9[ab]	18.0 ± 0.9[ab]	1130	42.5 ± 13.9	6.8 ± 1.0	13.1 ± 0.8
1200	54.8 ± 8.8	19.1 ± 2.6[ab]	18.3 ± 1.6[ab]	1200	43.8 ± 15.3	6.9 ± 1.0	13.4 ± 0.9
1230	61.6 ± 7.1	20.4 ± 2.9[ab]	19.4 ± 1.3[ab]	1230	40.7 ± 8.5	7.1 ± 1.0	13.1 ± 1.2
1300	54.7 ± 13.5	22.5 ± 3.3[ab]	19.8 ± 1.3[ab]	1300	38.1 ± 5.0	7.6 ± 0.8	13.1 ± 1.2

Conditions and calculations are as described in the text; n = 4 subjects studied under the two conditions. Values are means ± SD. Abbreviations: VLDL, very low density lipoprotein.

[a]Statistically significant difference versus pre-EtOH values.

[b]Statistically significant difference versus placebo treatment.

TABLE 4. The rate of appearance of plasma glycerol after EtOH or placebo treatment

Subject	Pre-EtOH	Post-EtOH	Pre-Placebo	Post-Placebo
		μmol/kg/min		
1	3.27	2.71	3.15	2.69
2	3.32	2.72	2.74	3.72
3	1.85	1.48	2.19	2.63
4	2.12	1.00	2.08	2.79
Mean ± SD	2.64 ± 0.72	1.98 ± 0.87	2.54 ± 0.50	2.96 ± 0.51

No statistically significant differences were observed.

in the EtOH study, the value of 11.0 ± 3.3 mg/kg per h was almost identical to that calculated with [2-$^{13}C_1$]glycerol.

DISCUSSION

The primary goal of this study was to characterize VLDL-TG production rates after the acute consumption of 48 g EtOH in normal volunteers using a new stable isotope method (incorporation of [2-$^{13}C_1$] glycerol into the glycerol moiety of VLDL-TG). Based on this method, there was no difference in VLDL-TG production rates after the consumption of EtOH or a placebo under overnight-fasted conditions. We also performed a pilot study comparing a previously described stable isotope technique for assessing VLDL-TG kinetics (incorporation of [1-$^{13}C_1$]acetate in VLDL-TG palmitate via the DNL pathway, references 17–19) to validate the [2-$^{13}C_1$]glycerol method. The two methods gave similar values for kinetic parameters. The consumption of EtOH also induced changes in glycerol metabolism, when compared with the placebo.

The consumption of 48 g EtOH elicited a modest (43%) but significant increase in plasma TG concentrations over 5 h compared to values after the placebo was consumed. Similar increases have been observed by others when similar doses of EtOH were administered (3). There may be a link between EtOH dose and plasma TG response, as other studies in which 2- to 3-times more EtOH was administered over 8–12 h reported increases in plasma TG concentrations of 65–75% (2, 4).

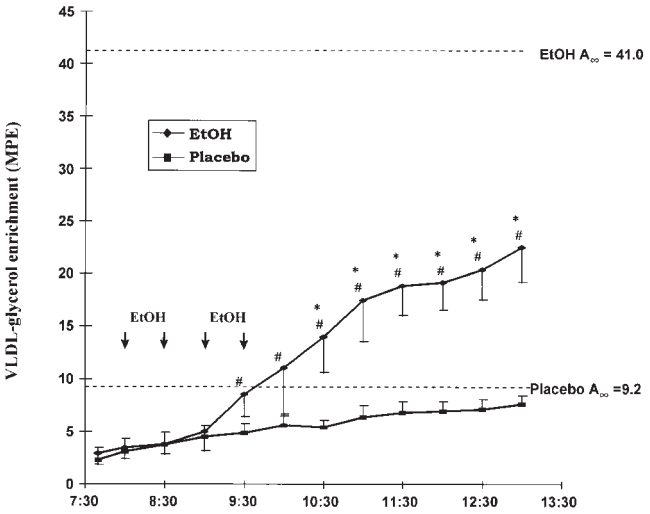

Fig. 4. VLDL-glycerol enrichments after EtOH or placebo. Predicted plateau values (A_∞) for EtOH and placebo values are represented by dotted lines; *statistically significant difference between treatments; #statistically significant difference vs. pre-treatment values.

TABLE 5. Calculation of triose-phosphate enrichments by MIDA of plasma glucose after the consumption of 48 g EtOH or a placebo

Treatment, Subject	M_1	M_2	ΔA_1	ΔA_2	p
Pre-Placebo					
1	0.1654	0.0310	0.0302	0.0068	0.113
2	0.1710	0.0316	0.0313	0.0071	0.115
3	0.1798	0.0355	0.0430	0.0108	0.145
4	0.1759	0.0338	0.0376	0.0090	0.131
Post-Placebo					
1	0.1765	0.0337	0.0409	0.0093	0.119
2	0.1828	0.0344	0.0431	0.0099	0.118
3	0.1902	0.0378	0.0534	0.0131	0.145
4	0.1922	0.0378	0.0548	0.0130	0.131
Pre-EtOH					
1	0.1760	0.0325	0.0388	0.0085	0.105
2	0.1899	0.0359	0.0508	0.0116	0.118
3	0.1696	0.0325	0.0335	0.0078	0.124
4	0.1747	0.0335	0.0383	0.0088	0.119
Post-EtOH					
1	0.1731	0.0338	0.0360	0.0095	0.184
2	0.1914	0.0393	0.0523	0.0148	0.181
3	0.1915	0.0412	0.0550	0.0164	0.199
4	0.1887	0.0404	0.0526	0.0158	0.199

Conditions and calculations are as described in the text. Pre- and post-treatment values represent steady-state values over time. Precursor enrichment (p) was calculated from the $\Delta A_2/\Delta A_1$ ratio using the best-fit regression equation $p = 4.395402\ (\Delta A_2/\Delta A_1)^4 + 7.255927\ (\Delta A_2/\Delta A_1)^3 - 5.614699\ (\Delta A_2/\Delta A_1)^2 + 2.913523\ (\Delta A_2/\Delta A_1) - 0.3299835$ (ref. 22). Abbreviations used: M_1, M_{+1} isotopomer; M_2, M_{+2} isotopomer; ΔA_1, change in fractional abundance of M_{+1} isotopomer (also called EM_1 elsewhere; refs. 23, 29); ΔA_2, change in fractional abundance of M_{+2} isotopomer (also called EM_2 elsewhere; refs. 23, 29). Precursor enrichments are expressed here as fractions

In the absence of dietary TG input, plasma TG concentrations are determined by rates of hepatic VLDL-TG production and the efficiency of TG clearance from the plasma. In the current study, we did not observe any significant differences in VLDL-TG production when 48 g EtOH or a placebo was consumed (Table 2). We have previously reported VLDL-TG production rates of 7.5 mg/kg per h after the consumption of 24 g EtOH (17) but had no control placebo protocol for comparison. In the present study, we observed slightly higher values (11.9 mg/kg per h EtOH, 14.7 mg/kg per h placebo). The rates of VLDL-TG production that we measured in the present study are similar to the 12–14 mg/kg per h measured in normal overnight-fasted subjects by others (12, 32) and are lower than those reported for hypertriglyceridemic patients (20–24 mg/kg per h, references 11, 12). As plasma TG concentrations increased 43% but VLDL-TG production rates did not change after EtOH consumption, reduced VLDL-TG clearance must account for elevations in plasma TG when EtOH was consumed (Table 2).

One technical issue that deserves comment relates to the measurement of VLDL-TG kinetics in the non-steady state after EtOH consumption. A non-steady state in plasma TG concentrations was observed after EtOH (Fig.

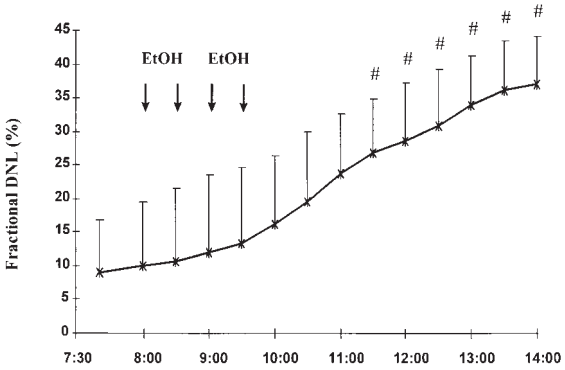

Fig. 5. Fractional de novo lipogenesis (DNL) after 48 g EtOH. These results are only from subjects 5–7 who received [1-$^{13}C_1$]acetate. Calculated mean intrahepatic acetyl-CoA precursor enrichments were 0.092 ± 0.013 M.E. pre-EtOH and 0.041 ± 0.004 M.E. post-EtOH; [#] statistically significant difference vs. pre-treatment values.

3), and is unavoidable experimentally here, unless one maintained high plasma EtOH concentrations for 12–16 h prior to beginning the isotope infusion; this, of course, would be difficult to justify in human subjects on ethical grounds. Formal kinetic analysis demonstrates that the metabolic cause of the non-steady state (increased production rate or reduced clearance efficiency) can nevertheless be established from an isotope labeling experiment, as was performed here. A brief mathematical discussion of this point follows (see ref. 33 for a more extensive discussion).

The accumulation of label in a product during an endogenous labeling experiment is described by the following general equation:

$$dB^*/dt = (k_s \times A^*) - (k_d \times B^*) \qquad Eq.\ 1)$$

where B* = isotope enrichment of product B, A* = isotope enrichment of precursor A, k_d = fraction of B removed per unit time (d^{-1}), and k_s = fraction of B replaced by synthesis from A per unit time (= production rate/pool size, units d^{-1}). If a metabolic steady state is present, $k_s = k_d = k$, and,

$$dB^*/dt = k\,(A^* - B^*). \qquad Eq.\ 2)$$

This is the standard kinetic equation (in its differential form) and results in straightforward experimental labeling results in the steady state: reduced clearance (lower k) obviously results in slower accumulation of label in B. Indeed, if A* is known, dB*/dt is directly proportional to k, so that the rate of label accumulation directly reflects k.

If a non-steady state is present, $k_s \neq k_d$. An increase in the pool size must reflect either *A*) higher production rate, or *B*) lower clearance efficiency. If situation *A*) exists (production is higher and clearance is unchanged), the 'k_s' is by definition higher early, before steady state is reached (k_s = production rate/pool size, and pool size has not yet reached its steady state value). Accumulation of labeled B* will therefore be accelerated since $k_s \times A^*$ in equation 1 is higher while $k_d \times B^*$ lags until B* is highly labeled. Accordingly, increased production will indeed result experimentally in a more rapidly labeled product and can be interpreted in this manner.

Alternatively, if situation *B*) exists (clearance is reduced and production is unchanged), then 'k_s' is by definition lower from the beginning and up to the new steady state (k_s = production/pool size, and pool size increases). Accumulation of labeled B* will therefore tend to be somewhat slower, as $k_s \times A^*$ in equation 1 is lower, while $k_d \times$

TABLE 6. Calculation of de novo lipogenesis by MIDA after the consumption of 48 g EtOH

Time	ΔA_1	ΔA_2	Ratio ($\Delta A_1/\Delta A_2$)	p	DNL Contribution
					%
Subject 5					
0740	0.0356	0.0182	0.5098	0.0629	17
0800	0.0420	0.0213	0.5073	0.0625	20
0830	0.0471	0.0241	0.5115	0.0632	22
0900	0.0501	0.0248	0.4941	0.0601	24
0930	0.0513	0.0249	0.4845	0.0583	25
1000	0.0522	0.0240	0.4604	0.0538	27
1030	0.0549	0.0234	0.4269	0.0475	31
1100	0.0570	0.0232	0.4071	0.0437	34
1130	0.0576	0.0226	0.3923	0.0408	36
1200	0.0598	0.0229	0.3830	0.0389	38
1230	0.0608	0.0227	0.3731	0.0370	40
1300	0.0607	0.0221	0.3649	0.0353	41
1330	0.0610	0.0215	0.3526	0.0329	44
1400	0.0622	0.0221	0.3546	0.0333	45
Subject 6					
0740	0.0036	0.0021	0.5788	0.0751	2
0800	0.0035	0.0021	0.5836	0.0759	2
0830	0.0035	0.0022	0.6365	0.0849	1
0900	0.0048	0.0025	0.5141	0.0637	2
0930	0.0064	0.0031	0.4804	0.0575	3
1000	0.0116	0.0046	0.3940	0.0411	7
1030	0.0167	0.0065	0.3920	0.0407	10
1100	0.0242	0.0085	0.3501	0.0324	18
1130	0.0304	0.0106	0.3482	0.0320	22
1200	0.0317	0.0108	0.3398	0.0303	24
1230	0.0351	0.0120	0.3413	0.0306	27
1300	0.0402	0.0134	0.3330	0.0289	32
1330	0.0438	0.0148	0.3377	0.0298	34
1400	0.0458	0.0155	0.3382	0.0299	36
Subject 7					
0740	0.0177	0.0119	0.6736	0.0910	7
0800	0.0189	0.0125	0.6619	0.0891	8
0830	0.0182	0.0121	0.6648	0.0896	7
0900	0.0202	0.0121	0.5996	0.0787	9
0930	0.0222	0.0118	0.5301	0.0666	10
1000	0.0268	0.0127	0.4747	0.0565	13
1030	0.0310	0.0138	0.4456	0.0510	17
1100	0.0347	0.0149	0.4303	0.0481	19
1130	0.0376	0.0157	0.4191	0.0460	21
1200	0.0391	0.0163	0.4170	0.0456	22
1230	0.0430	0.0179	0.4159	0.0454	25
1300	0.0476	0.0199	0.4185	0.0459	27
1330	0.0515	0.0214	0.4151	0.0452	30
1400	0.0537	0.0225	0.4198	0.0461	30

Conditions and calculations are as described in the text. The rise in % DNL contributed over time was modeled to calculate VLDL-TG kinetics (Fig. 5, Table 7). Precursor enrichment for DNL (p) was calculated from the $\Delta A_2/\Delta A_1$ ratio using the palmitate methyl ester best fit regression equation $p = 0.01578508\ (\Delta A_2/\Delta A_1)^3 - 0.08572153\ (\Delta A_2/\Delta A_1)^2 + 0.2561532\ (\Delta A_2/\Delta A_1) - 0.04748384$ (refs. 28–30). Percent DNL was calculated using the value of p determined, as described previously (28–30). Abbreviations: ΔA_1, change in fractional abundance of M_{+1} isotopomer compared to baseline; ΔA_2, change in fractional abundance of M_{+2} isotopomer compared to baseline; ratio, ratio of $\Delta A_2/\Delta A_1$; DNL, de novo lipogenesis.

TABLE 7. Comparison between kinetics calculated from [2-$^{13}C_1$]glycerol incorporation (into VLDL-glycerol) and [1-$^{13}C_1$]acetate incorporation (into VLDL-palmitate)

	EtOH [2-$^{13}C_1$]Glycerol Incorporation		EtOH [1-$^{13}C_1$]Acetate Incorporation	
Subject	K_s	$t_{1/2}$	K_s	$t_{1/2}$
	h^{-1}	h	h^{-1}	h
5	0.28	2.45	0.27	2.51
6	0.19	3.64	0.20	3.38
7	0.14	4.88	0.12	5.93
Mean	0.20	3.63	0.20	3.94
±SD	0.07	1.35	0.08	1.78

Conditions and calculations are as described in the text. Individual data compare K_s and $t_{1/2}$ in subjects who received both [2-$^{13}C_1$]glycerol and [1-$^{13}C_1$]acetate. Values are given as mean ± SD. No statistically significant differences were observed between EtOH and placebo treatments for any of the parameters listed. Abbreviations: K_s, synthetic constant; $t_{1/2}$, half-life; VLDL, very low density lipoprotein.

B* does not have an impact until B* becomes significantly labeled. So, reduced clearance will result experimentally in a less rapidly labeled product and can be interpreted accordingly. The take-home message is that directional changes in label accumulation rate in B* will indeed reveal the kinetic mechanism responsible for the change in pool size (production or clearance), in at least a semiquantitative manner.

Several investigators have measured VLDL-TG production rates in response to acute (13, 14, 16) or chronic (15, 34) EtOH exposure. When VLDL-TG production was measured in response to acute EtOH consumption in normal volunteers, increased rates were observed by some (14, 16) but not by others (13, 16). In a study by Crouse and Grundy (13), normal subjects did not have any differences in VLDL-TG production rates when EtOH was included in fat-free meals; EtOH induced a 45% increase in several obese subjects, however. Wolfe et al. (16) reported that EtOH increased VLDL-TG production above pre-EtOH levels when normal subjects had fasted 69 h but not after a 15-h fast. The increased VLDL-TG production in the 69-h fasted subjects was apparently linked with increased peripheral release of FFA, as both FFA flux and FFA concentrations were increased over baseline levels following EtOH infusion in the 69-h fasted group but not the 15-h fasted group. It is possible that the stress induced by the induction of hypoglycemia stimulated a catecholamine response and subsequently overcame the usual antilipolytic effect of acetate (35–38) and increased peripheral lipolysis (39) in the 69-h fasted subjects. The increased VLDL-TG production after EtOH observed by Wolfe et al. (16) in 69-h fasted individuals and by Crouse and Grundy (13) in obese subjects may have been driven by increased lipolytic rates.

Lipolysis was inhibited non-significantly by EtOH consumption in the present study, as measured by the rate of appearance of glycerol. The rate of appearance of glycerol was assessed by quantifying enrichments (Table 4) of plasma glycerol. While the quantity of [2-$^{13}C_1$] glycerol administered gave enrichments above what could be considered a "tracer" dose, we have elsewhere found no effect on calculated lipolytic rates when adding large doses of [2-$^{13}C_1$] glycerol to tracer doses of [$^2H_5$] glycerol (A. Basinger, R. A. Neese, M. K. Hellerstein, unpublished data). After EtOH consumption, we observed a 24% decrease in plasma glycerol flux (Table 4); this is similar to the decrease we observed after the consumption of 24 g EtOH previously (17). While we did not measure FFA flux in the current study, FFA flux has been demonstrated by us (17) and others (14, 16, 40) to be reduced after moderate EtOH consumption. Thus, hepatic VLDL-TG production after EtOH was likely kept in check by the suppression of peripheral lipolysis.

The modeling of [2-$^{13}C_1$] glycerol incorporation into VLDL-TG after EtOH intake (Fig. 4) is based on the assumption of a relatively stable enrichment in the intracellular precursor pool, α-glycerol phosphate. If intrahepatic α-glycerol phosphate enrichments are not constant during the post-EtOH period (0800–1300), fitting the data to a simple exponential that approaches an asymptotic value would not be appropriate. If, for example, α-glycerol phosphate enrichments slowly increased during the hours after EtOH consumption, using the asymptotic VLDL-glycerol value to represent the intracellular precursor pool enrichment during the entire period would result in an overestimation of precursor enrichment and an underestimation of true K_s (27). Because effects of EtOH on the hepatic redox state occur rapidly (41), however, the enrichments of the intrahepatic α-glycerol phosphate and triose-phosphate pools should rapidly achieve their steady-state values. Comparison of the incorporation kinetics of [2-$^{13}C_1$]glycerol and [1-$^{13}C_1$]acetate into VLDL-TG strongly supports this assumption; the nearly identical K_s and VLDL-TG production rates that were calculated by these independent methods in the same individuals (Table 7) make it unlikely that the glycerol labeling method is subjected to a changing intracellular precursor enrichment.

The maximal VLDL-glycerol enrichments after EtOH were several times higher than the highest measured values after the placebo (Table 3, Fig. 4). Peak VLDL-glycerol enrichments reflect intrahepatic α-glycerol phosphate labeling and any residual dilution from unlabeled TG in VLDL. Thus, EtOH either alters the intrahepatic α-glycerol phosphate pool enrichment or the contribution of newly assembled TG to circulating VLDL. In animal systems, intrahepatic α-glycerol phosphate concentrations increase when EtOH is given (42–44). The biochemical mechanism involves the altered hepatic redox state associated with EtOH oxidation (45, 46). Nicotinamide adenine dinucleotide (NAD) is required as a co-substrate (Fig. 1) for conversion of α-glycerol phosphate to dihydroxyacetone phosphate (DHAP) via the enzyme glycerol 3-phosphate dehydrogenase (G3PDH). The obligatory oxidation of EtOH by alcohol dehydrogenase (Fig. 1) limits the availability of NAD; our results suggest that the rate of conversion of α-glycerol phosphate to DHAP may thereby be reduced.

These results also provide indirect evidence for reduced flux of α-glycerol phosphate to DHAP during hepatic EtOH oxidation. Under fasting conditions (as with the pla-

cebo protocol), the VLDL-glycerol enrichments reached only about 60% of the calculated intrahepatic triose phosphate enrichments (Table 3). The extrapolated plateau VLDL-glycerol enrichments (A_0 = 9.2%) from modeling of the incorporation curve were reasonably close to the triose-phosphate enrichments calculated by MIDA of plasma glucose (12.7%). In contrast, both the VLDL-glycerol and hepatic triose-phosphate enrichments were higher when EtOH was given; the VLDL-glycerol enrichments rose to levels greater than the hepatic triose-phosphate enrichment. Extrapolated maximum values of VLDL-TG glycerol (A_∞ = 41.0%) were even higher post-EtOH and were almost 2-fold greater than hepatic triose-phosphate enrichments (Table 3). These results suggest an accumulation of labeled glycerol at G3PDH (Fig. 1), i.e., an isotopic gradient between hepatic α-glycerol phosphate and DHAP.

It is interesting to note that the highest VLDL-glycerol enrichments that we observed post-EtOH were still at most one-half to one-third of the plasma glycerol enrichments (Table 3), and even the asymptotic enrichments predicted by kinetic modeling of the VLDL-glycerol curves were still <65% of the plasma glycerol enrichment. Hepatic α-glycerol phosphate must therefore derive at least in part from other sources besides plasma glycerol. Reshef, Hanson, and Ballard (47) have discussed "glycero-neogenesis," or the synthesis of α-glycerol phosphate from gluconeogenic precursors. We did not determine the metabolic source responsible for the dilution between plasma glycerol and α-glycerol phosphate, but studies in cell systems (48) suggest that flux from DHAP to α-glycerol phosphate may have contributed.

In conclusion, consumption of 48 g EtOH increases plasma TG concentrations but does not increase VLDL-TG production rates in normal healthy men when measured by modeling of [2-$^{13}C_1$]glycerol incorporation into VLDL-glycerol. [2-$^{13}C_1$]glycerol incorporation into VLDL-glycerol gave kinetic results similar to concurrent [1-$^{13}C_1$] acetate incorporation into the palmitate moiety of VLDL. Finally, EtOH causes an accumulation of labeled glycerol in the hepatic α-glycerol phosphate pool, which is likely mediated by hepatic redox changes associated with EtOH oxidation.

This work was supported in part by NIAAA grant 1 RO3 AA10693-01 and NIH grant RR-00083 from the Division of Research Resources for the General Clinical Research Center. We gratefully acknowledge Drs. Mark Christiansen, Peter Linfoot, Mark Hudes, and Lisa Lim for their contributions to this study. We also acknowledge the nurses in the San Francisco General Hospital GCRC for their help.

Manuscript received 3 November 1997, in revised form 27 May 1998, and in re-revised form 18 August 1998.

REFERENCES

1. Avogaro, P., and G. Cazzolato. 1975. Changes in the composition and physio-chemical characteristics of serum lipoproteins during ethanol-induced lipaemia in alcoholic subjects. *Metabolism.* **24:** 1231–1242.
2. Jones, D. P., M. S. Losowsky, C. S. Davidson, and C. S. Lieber. 1963. Effects of ethanol on plasma lipids in man. *J. Lab. Clin. Med.* **62:** 675–682.
3. Kaffarnik, H., and J. Schneider. 1970. Zur kurzfristegen wirkung des athylalkohols auf die serumlipide gesunder fastender versuchspersonen. *Z. Ges. Exp. Med.* **152:** 187–200.
4. Kaffarnik, H., J. Schneider, R. Schubotz, L. Hausmann, G. Muhlfellner, O. Muhlfellner, and P. Zofel. 1978. Plasma lipids, triglyceride/fatty acid pattern, and plasma insulin in fasted healthy volunteers during continuous ingestion of ethanol. *Atherosclerosis.* **29:** 1–7.
5. Taskinen, M. R., and E. A. Nikkila. 1977. Nocturnal hypertriglyceridemia and hyperinsulinemia following moderate evening intake of alcohol. *Acta Med. Scand.* **202:** 173–177.
6. Castelli, W. P., T. Gordon, M. C. Hjortland, A. Kagan, J. T. Doyle, C. G. Hames, S. B. Hulley, and W. J. Zukel. 1977. Alcohol and blood lipids. *Lancet.* **2:** 153–155.
7. Chait, A., M. Mancini, A. W. February, and B. Lewis. 1972. Clinical and metabolic study of alcoholic hyperlipidemia. *Lancet.* **2:** 62–64.
8. Jenkins, P. J., R. W. Harper, and P. J. Nestel. 1978. Severity of coronary atherosclerosis related to lipoprotein concentrations. *Br. Med. J.* **2:** 388–391.
9. Gaziano, J. M., J. E. Buring, J. L. Breslow, S. Z. Goldhaber, B. Rosner, M. VanDenburgh, W. Willett, and C. H. Hennekens. 1993. Moderate alcohol intake, increased levels of high-density lipoprotein and its subfractions, and decreased risk of myocardial infarction. *N. Engl. J. Med.* **329:** 1829–1834.
10. Thun, M. J., R. Peto, A. D. Lopez, J. H. Monaco, S. J. Henly, C. W. Heath, and R. Doll. 1997. Alcohol consumption and mortality among middle-aged and elderly U.S. adults. *N. Engl. J. Med.* **337:** 1705–1714.
11. Harris, W. S., W. E. Connor, R. Illingworth, D. W. Rothrock, and D. M. Foster. 1990. Effects of fish oil on VLDL triglyceride kinetics in humans. *J. Lipid Res.* **31:** 1549–1558.
12. Olefsky, J., J. W. Farquhar, and G. M. Reaven. 1974. Sex differences in the kinetics of triglyceride metabolism in normal and hypertriglyceridaemic human subjects. *Eur. J. Clin. Invest.* **4:** 121–127.
13. Crouse, J. R., and S. M. Grundy. 1984. Effects of alcohol on plasma lipoproteins and cholesterol and triglyceride metabolism in man. *J. Lipid Res.* **25:** 486–496.
14. Nestel, P. J., and E. Z. Hirsch. 1965. Mechanism of alcohol-induced hypertriglyceridemia. *J. Lab. Clin. Med.* **66:** 357–365.
15. Sane, T., E. A. Nikkila, M. R. Taskinen, M. Valimaki, and R. Ylikahri. 1984. Accelerated turnover of very low density lipoprotein triglycerides in chronic alcohol users. *Atherosclerosis.* **531:** 185–193.
16. Wolfe, B. M., J. R. Havel, E. B. Marliss, J. P. Kane, J. Seymour, and S. P. Ahuja. 1976. Effects of a 3-day fast and of ethanol on splanchnic metabolism of FFA, amino acids, and carbohydrates in healthy young men. *J. Clin. Invest.* **57:** 329–340.
17. Siler, S. Q., R. A. Neese, and M. K. Hellerstein. 1997. Effects of ethanol consumption on lipolysis, de novo lipogenesis, and acetate in humans. *FASEB J.* **11:** A140.
18. Schwarz, J. M., R. A. Neese, S. Turner, D. Dare, and M. K. Hellerstein. 1995. Short-term alterations in carbohydrate energy intake in humans. *J. Clin. Invest.* **96:** 2735–2743.
19. Aarsland, A., D. Chinkes, and R. R. Wolfe. 1996. Contributions of de novo synthesis of fatty acids to total triglyceride secretion during prolonged hyperglycemia/hyperinsulinemia in normal men. *J. Clin. Invest.* **98:** 2008–2017.
20. Hellerstein, M. K, R. A. Neese, J. M. Schwarz, S. Turner, D. Faix, and K. Wu. 1997. Altered fluxes responsible for reduced hepatic glucose production and gluconeogenesis by exogenous glucose in rats. *Am. J. Physiol.* **272:** E163–E172.
21. Hellerstein, M. K., R. A. Neese, P. Linfoot, M. Christiansen, S. Turner, and A. Letscher. 1997. Hepatic gluconeogenesis fluxes and glycogen turnover during fasting in humans. A stable isotope study. *J. Clin. Invest.* **100:** 1305–1319.
22. Neese, R. A., J. M. Schwarz, D. Faix, S. Turner, A. Letscher, D. Vu, and M. K. Hellerstein. 1995. Gluconeogenesis and intrahepatic triose phosphate flux in response to fasting or substrate loads. Application of the mass isotopomer distribution analysis technique with testing of assumptions and potential problems. *J. Biol. Chem.* **270:** 14452–14466.
23. Hellerstein, M. K., K. Wu, S. Kaempfer, C. Kletke, and C. H. L. Shackleton. 1991. Sampling the lipogenic hepatic acetyl-CoA pool in vivo in the rat. Comparison of xenobiotic probe to values predicted from isotopomeric distribution in circulating lipids and measurement of lipogenesis and acetyl-CoA dilution. *J. Biol. Chem.* **266:** 10912–10919.
24. Folch, J., M. Lees, and G. Sloane Stanley. 1957. A simple method

for the isolation and purification of total lipids from animal tissue. *J. Biol. Chem.* **226:** 497–509.
25. Shen, B. W., A. M. Scanu, and F. J. Kezdy. 1977. Structure of human serum lipoproteins inferred from compositional analysis. *Proc. Natl. Acad. Sci. USA.* **74:** 837–841.
26. Neese, R. A., N. L. Benowitz, R. Hoh, D. Faix, A. LaBua, K. Pun, and M. K. Hellerstein. 1994. Metabolic interactions between surplus dietary energy intake and cigarette smoking or its cessation. *Am. J. Physiol.* **267:** E1023–E1034.
27. Wolfe, R. R. 1992. Radioactive and Stable Isotope Tracers in Biomedicine: Principles and Practice of Kinetic Analysis. Wiley–Liss, New York, NY. 119–144.
28. Faix, D., R. Neese, C. Kletke, S. Wolden, D. Cesar, M. Coutlangus, C. H. L. Shackleton, and M. K. Hellerstein. 1993. Quantification of menstrual and diurnal periodicities in rates of cholesterol and fat synthesis in humans. *J. Lipid Res.* **34:** 2063–2075.
29. Hellerstein, M. K., M. Christiansen, S. Kaempfer, C. Kletke, K. Wu, J. S. Reid, K. Mulligan, N. S. Hellerstein, and C. H. L. Shackleton. 1991. Measurement of de novo hepatic lipogenesis in humans using stable isotopes. *J. Clin. Invest.* **87:** 1841–1852.
30. Hellerstein, M. K. 1995. Methods for the measurement of fatty acid and cholesterol metabolism. *Curr. Opin. Lipidol.* **6:** 172–181.
31. Hellerstein, M. K., and R. A. Neese, 1992. Mass isotopomer distribution analysis: a technique for measuring biosynthesis and turnover of polymers. *Am. J. Physiol.* **263:** E988–E1001.
32. Grundy, S. M., H. Y. I. Mok, L. Zech, D. Steinberg, and M. Berman. 1979. Transport of very low density lipoprotein triglycerides in varying degrees of obesity and hypertriglyceridemia. *J. Clin. Invest.* **63:** 1274–1283.
33. Waterlow, J. C., P. J. Garlick, and D. J. Millward. 1978. Protein Turnover in Mammalian Tissues and in the Whole Body. Amsterdam, North Holland. 217–219.
34. Savolainen, M. J., E. Baraona, M. A. Leo, and C. S. Lieber. 1986. Pathogenesis of the hypertriglyceridemia at early stages of alcoholic liver injury in the baboon. *J. Lipid Res.* **27:** 1073–1083.
35. Abramson, E. A., and R. A. Arky. 1968. Acute antilipolytic effects of ethyl alcohol and acetate in man. *J. Lab. Clin. Med.* **72:** 105–117.
36. Crouse, J. R., C. D. Gerson, L. M. DeCarli, and C. S. Lieber. 1968. Role of acetate in the reduction of plasma free fatty acids produced by ethanol in man. *J. Lipid Res.* **9:** 509–512.
37. Nilsson, N. O., and P. Belfrage. 1978. Effects of acetate, acetaldehyde, and ethanol on lipolysis in isolated rat adipocytes. *J. Lipid Res.* **19:** 737–741.
38. Yki-Jarvinen, H., V. A. Koivisto, R. Ylikahri, and M. R. Taskinen. 1988. Acute effects of ethanol and acetate on glucose kinetics in normal subjects. *Am. J. Physiol.* **254:** E175–E180.
39. Galster, A. D., W. E. Clutter, P. E. Cryer, J. A. Collins, and D. M. Bier. 1981. Epinepherine plasma thresholds for lipolytic effects in man. *J. Clin. Invest.* **67:** 1729–1738.
40. Jones, D. P., E. S. Perman, and C. S. Lieber. 1965. Free fatty acid turnover and triglyceride metabolism after ethanol ingestion in man. *J. Lab. Clin. Med.* **66:** 804–813.
41. Krebs, H. A., R. A. Freedland, R. Hems, and M. Stubbs. 1969. Inhibition of hepatic gluconeogenesis by ethanol. *Biochem. J.* **112:** 117–124.
42. Brauer, M., and M. F. Ling. 1991. The effects of chronic ethanol consumption on the intact rat liver studied by in vivo ^{31}P NMR spectroscopy. *Magnet. Reson. Med.* **20:** 100–112.
43. Masson, S., F. Desmoulin, M. Sciaky, and P. J. Cozzone. 1992. The effects of ethanol concentration of glycero-3-phosphate accumulation in the perfused rat liver. *Eur. J. Biochem.* **205:** 187–194.
44. Nikkila, E. A., and K. Ojala. 1963. Role of hepatic l-α-glycerophosphate and triglyceride synthesis in the production of fatty liver by ethanol. *Proc. Soc. Exp. Biol. Med.* **113:** 814–817.
45. Cronholm, T., and T. Curstedt. 1984. Heterogeneity of the *sn*-glycerol 3-phospate pool in isolated hepatocytes, demonstrated by the use of deuterated glycerols and ethanol. *Biochem. J.* **224:** 731–739.
46. Lieber, C. S. 1991. Hepatic, metabolic, and toxic effects of ethanol: 1991 update. *Alcohol. Clin. Exp.* **15:** 573–592.
47. Reshef, L., R. W. Hanson, and F. J. Ballard. 1969. Glyceride-glycerol synthesis from pyruvate. *J. Biol. Chem.* **244:** 1994–2001.
48. Yu, B. Y., and T. Cronholm. 1997. Coupling of ethanol metabolism to lipid biosynthesis: labelling of the glycerol moieties of *sn*-glycerol-3-phosphate, a phosphatidic acid and a phosphatidylcholine in liver or rats given [1,1-$^{2}H_2$] ethanol. *Biochim. Biophys. Acta.* **1344:** 165–170.